Gene expression in sexually dimorphic muscles in sheep[1]

R. G. Mateescu[2] and M. L. Thonney

Department of Animal Science, Cornell University, Ithaca, NY 14853

ABSTRACT: Testosterone is known to act differentially on skeletal muscle from different regions of the body. Two genes likely to mediate the testosterone effect are insulin-like growth factor I (IGF-I), an important growth regulator acting in an autocrine and paracrine way, and androgen receptor (AR), because receptor density could account for differential muscle growth. Another muscle-specific gene that may play a role in differential muscle growth is myostatin, a member of the transforming growth factor-beta superfamily, shown to be a negative regulator of skeletal muscle mass. The objective of this study was to quantify and compare the steady state expression of these three genes in two different skeletal muscles in sheep. Eleven Dorset rams were slaughtered after reaching puberty and total RNA was extracted from samples of semitendinosus and splenius muscles. Insulin-like growth factor I mRNA was measured using a competitive reverse-transcription-polymerase chain reaction. Androgen receptor and myostatin mRNA were measured by a ribonuclease protection assay (RPA) with standard curves. The means (attomoles/μg RNA) for splenius and semitendinosus muscles were 1.39 and 1.02 (SE = 0.14), 4.05 and 2.96 (SE = 0.24), and 4.30 and 3.85 (SE = 0.37) for IGF-I, AR, and myostatin, respectively. The difference between the two muscles was significant for IGF-I and AR mRNA levels with higher levels in the splenius but not significant for myostatin. Our results show that locally produced IGF-I and the regulation of AR expression may be important for sexually dimorphic muscle growth patterns.

Key Words: Gene Expression, Muscles, Sheep

 J. Anim. Sci. 2002. 80:1879–1887

Introduction

Sexual dimorphism in muscle growth is related to the protein anabolic effect of testicular hormones. Splenius muscle in rams and wethers implanted with testosterone was heavier and had a biphasic growth pattern compared to the single phase of growth of the same muscle in wethers (Arnold et al., 1997). Among insulin-like growth factor I (**IGF-I**), growth hormone and cortisol, only IGF-I plasma concentrations increased in response to the testosterone treatment (Arnold et al., 1996). Although it was shown that testosterone was responsible for differential growth of certain muscle groups, a conclusive explanation of the mechanism for this is lacking.

Testosterone could exert an effect on muscle growth through the IGF-I axes. Locally produced IGF-I is an important growth regulator acting in an autocrine and paracrine manner (Weimann and Kiess, 1990), but different muscles may possess different IGF-I sensitivities (Boge et al., 1995) and(or) IGF-I synthesis rates (Pfaffl et al., 1998b; Thissen et al., 1994) and, therefore, exhibit different growth rates. Also, testosterone action is mediated by the androgen receptor (**AR**), which transduces the steroid signal within cells. Different receptor densities, as postulated by Sauerwein and Meyer (1989), may account for relatively higher sensitivity to testicular steroids in the neck muscles. Testosterone could also regulate muscle-specific genes. One of these is myostatin, a gene shown to be a negative regulator of muscle mass.

The objective of this study was to elucidate the possible role of IGF-I, AR, and myostatin genes in differential growth. The approach was to quantify IGF-I, AR, and myostatin mRNA expression in splenius (a sexually dimorphic muscle) and semitendinosus (not a sexually dimorphic muscle) muscles in rams and to assess whether the levels of expression of these genes were different.

Materials and Methods

Animals

Eleven pubertal Dorset rams with ages ranging from 192 to 465 d with a mean and standard deviation of

[1]Supported in part by Cornell University Agricultural Experiment Hatch Project 433.

[2]Correspondence: 314 Morrison Hall (phone: 607-255-2851; fax: 607-255-9829; E-mail: rgm9@cornell.edu).

Received October 3, 2001.

Accepted February 21, 2002.

282.2 and 125.7 d, respectively, and weights ranging from 33 to 75 kg with a mean and standard deviation of 53 and 15 kg, respectively, were slaughtered. Samples from semitendinosus and splenius muscles and liver were collected within 15 min after exsanguination, snap-frozen in liquid nitrogen, and stored at –70°C until they were subsequently analyzed. Blood samples were collected at exsanguination; the tubes were placed on ice and centrifuged and the plasma was harvested and stored at –20°C until it was assayed.

Ribonucleic Acid Isolation

Total RNA was isolated using the guanidine thiocyanate, acid phenol:chloroform procedure of Chomczynski and Sacchi (ToTALLY RNA Total RNA Isolation Kit, Ambion, Austin, TX). Using a hand-held Tissue Tearor (Biospec Products, Bartlesville, OK), 140 mg of muscle tissue and 40 mg of liver tissue were homogenized on ice in denaturation solution. After isopropanol precipitation, RNA pellets extracted from liver were washed with LiCl to remove glycogen. The RNA pellet was resuspended in 40 to 50 μL (muscles) and 80 to 100 μL (liver) of 1 m*M* sodium citrate, pH 6.4 ± 0.2 (The RNA Storage Solution, Ambion). The concentration of RNA in the final preparations was calculated from the OD_{260}. The integrity of RNA was verified by denaturing agarose gel electrophoresis and ethidium bromide stain.

Testosterone Assay

Testosterone concentrations in plasma were determined in the Cornell Veterinary Medicine Diagnostic Laboratory using a radioimmunoassay method (Total Testosterone Coat-A-Count Kit, Diagnostic Products, Los Angeles, CA).

Ribonuclease Protection Assay

Preparation of the AR, Myostatin, GAPDH-Labeled Antisense and Unlabeled Sense Riboprobes. From 500 ng of total ovine muscle RNA, cDNA was generated using a gene-specific primer (Table 1) in the reverse transcription (Display THERMO-RT Kit, Display Systems Biotech, Boston, MA). Total RNA, 1× RT buffer, 0.5 m*M* dNTP (each of dATP, dGTP, dCTP, dTTP), 1 μ*M* reverse primer, and Display Terminator Mix were incubated for 40 min at 42°C followed by 10 min at 65°C. Specific regions were amplified from 1 μL of reverse trancription reaction in a 10-μL PCR amplification reaction (Table 1) using the Idaho Technologies Rapid Cycler (Idaho Falls, ID).

Each 10-μL reaction contained 1 μL of reverse trancription reaction, Idaho Technologies buffer (50 m*M* Tris, pH 8.3; 0.25 m*M* crystalline BSA; 2 m*M* or 4 m*M* $MgCl_2$ as shown in Table 1; and sucrose), 0.4 U *Taq* DNA polymerase (Gibco BRL, Rockville, MD), 0.2 m*M* dNTP (Promega, Madison, WI), and 0.5 μ*M* each primer. The 453-bp myostatin (GenBank accession number AF019622, Figure 1) and the 556-bp GAPDH (GenBank accession number U94889; Lee et al., 1998) PCR products were cloned into pCR II using a TA cloning kit (Invitrogen, Carlsbad, CA). The 910-bp oAR (GenBank accession number AF105713) PCR product was cloned into pCR 2.1.

The plasmids were subsequently transfected into INVαF′ competent cells (Stratagene, La Jolla, CA). Positive transformants were selected on the basis of ampicillin resistance and a selection of these were grown in LB broth containing ampicillin (50 μg/μL). The ovine cDNA structures for AR, myostatin, and GAPDH and the orientations in the plasmid were confirmed by sequencing. The myostatin and GAPDH PCR products were found to be in reverse sequence in the vector. The plasmids were named pCR(myostatin) and pCR(GAPDH) to designate cDNA templates for ovine myostatin, GAPDH, and pCR(ARs) and pCR(ARas) to designate cDNA templates for ovine AR sense and AR antisense (because the pCR 2.1 had only the T7 promoter, two plasmids were required, one for each orientation), respectively. Large-scale plasmid DNA purification was carried out using a Qiagen Plasmid Kit (Qiagen, Valencia, CA).

The vectors pCR(myostatin), pCR(ARs), and pCR(ARas) were linearized by *Bam*HI, *Bam*HI and *Hin*cII digestion, respectively, and the cloned ovine cDNA were transcribed with T7 RNA polymerase at 37°C for 1 h using the reagents supplied with the MaxiScript Kit (Ambion) to produce sense myostatin, sense AR, and antisense AR, respectively. The vectors pCR(myostatin) and pCR(GAPDH) were linearized by *Dra*I and *Eco*O109I digestion, respectively, and the cloned ovine cDNA were transcribed with SP6 RNA polymerase (Ambion) at 37–C for 1 h to produce antisense myostatin and antisense GAPDH. At the end of the reaction, 1 μL of RNase-free DNase I (10 U) was added and the reaction was incubated for 15 min at 37°C. Subsequently, all sense and antisense RNA transcripts were gel-purified and the concentration was calculated from the OD_{260} after gel elution. The antisense RNA transcripts were labeled with Psoralen-Biotin using the BrightStar Psoralen-Biotin Nonisotopic Labeling Kit (Ambion). Due to the abundance of GAPDH, the probe concentration was adjusted to generate a signal in the same range with the myostatin and AR signal. This adjustment was accomplished by mixing biotin-labeled and unlabeled GAPDH probe at a ratio of 1:25.

Ribonuclease Protection Assay. Forty micrograms of splenius and semitendinosus muscle total RNA were coprecipitated with 1 ng of myostatin, AR, and GAPDH riboprobes and hybridization was performed at 42°C overnight using the protocol and reagents supplied in the RPA III Kit (Ambion) as described in the standard procedure. The next day, the mixture was treated with an RNase cocktail (0.04 U of RNase A and 1.5 U of RNase T1) to degrade single-stranded RNA. The protected fragments were precipitated, the

Table 1. Primer pairs and the PCR conditions used in generating ovine androgen receptor (AR), myostatin (MSTN), glyceraldehyde-3-phosphate dehydrogenase (GAPDH), insulin-like growth factor-I (IGF-I), and IGF-I MIMIC

Amplified fragment	Size bp	Primer name	Primer sequence	$MgCl_2$, m*M*	PCR conditions
		AR			30s94°C;
AR	910	Forward	5′-GCC TGA TCT GTG GAG ATG AA-3′	2	30 cycles: 0s[a]94°C, 0s55°C, 20s72°C;
		Reverse	5′-AGC TTG GTG AGC TGG TAG AA-3′		1min72°C; 5min25°C
		MSTN			30s94°C;
MSTN	453	Forward	5′-GCT CCT TGG AAG ACG ATG AC-3′	4	30 cycles: 0s94°C, 0s62°C, 20s72°C;
		Reverse	5′-CTT CTA AAA AAG GAT TCA GT-3′		1min72°C; 5min25°C
		GAPDH			30s94°C;
GAPDH	556	Forward	5′-C TGC ACC ACC AAC TGC TTA G-3′	2	30 cycles: 0s94°C, 0s55°C, 20s72°C;
		Reverse	5′-T TAC TCC TTG GAG GCC ATG T-3′		1min72°C; 5min25°C
		IGF-I			30s94°C
IGF-I	358	Forward	5′-CGC ATC TCT TCT ATC TGG CC-3′	4	30cycles: 0s94°C, 0s55°C, 20s72°C;
		Reverse	5′-TTG TTT CCT GCA CTC CCT CT-3′		1min72°C; 5min25°C
		IGFGAPDH			30s94°C
IGF-I MIMIC	325	Forward	5′-CGC ATC TCT TCT ATC TGG CCC TGC ACC ACC AAC TGC TTA G-3′	2	30 cycles: 0s94°C, 0s58°C; 20s72°C; 1min72°C; 5min25°C
		Reverse	5′-TTG TTT CCT GCA CTC CCT CTT TAC TCC TTG GAG GCC ATG T-3′		

[a]The denaturing and annealing temperatures were reached without setting a hold time because both denaturing and annealing occur almost instantaneously after the sample reached the appropriate temperature.

pellets were washed once with 75% ethanol, dried, resuspended in 10 μL of gel-loading buffer, denatured at 95°C for 5 min, loaded onto a 6% polyacrylamide/8M urea denaturing gel and run at 200V for approximately 1 h. The RNA was then electrophoretically transferred to a positively charged nylon membrane (Bright Star-Plus, Ambion) using a mini-gel blotting apparatus (BioRad, Hercules, CA) and 1× TBE as transfer buffer. The transfer was carried out for 1 h at 100 mA, and the membrane was UV-irradiated to crosslink the RNA to the nylon. The BrightStar BioDetection Kit (Ambion) was used for chemiluminescent detection of the protected fragments. At the end of the procedure, the membrane was exposed to x-ray film (Kodak) overnight at room temperature and for shorter periods (between 15 and 30 min) the following day.

Quantitative Analysis of Myostatin and AR mRNA. Known amounts (60, 40, 27, 18, 12, and 8 pg) of in vitro synthesized myostatin and AR sense RNA were hybridized with an excess of labeled antisense probe (1 ng) in RPA to construct standard curves. The values were plotted as the log of the amount of sense RNA vs the intensity of the protected band in the standard curve. The absolute amount of the protected RNA species in the muscle sample RNA was determined by comparing the intensity of the band to the standard curve, after correcting for the size difference and for the RNA loading difference. The protected fragments in the experimental samples differed in size from the protected fragments in the standard curve; therefore, the difference in the incorporation of biotin had to be taken into account. The following equation was used to correct for size difference:

$$\text{Corrected (band density)} = \text{band density} \times \frac{\text{protected fragment in the standard curve (bp)}}{\text{protected fragment in the experimental samples (bp)}}$$

To correct for variations in RNA loading, the band densities (corrected for size differences) were multiplied by the ratio between the strongest GAPDH band (considered to correspond to the 40 μg RNA loaded into the gel) and the GAPDH band from the respective lane.

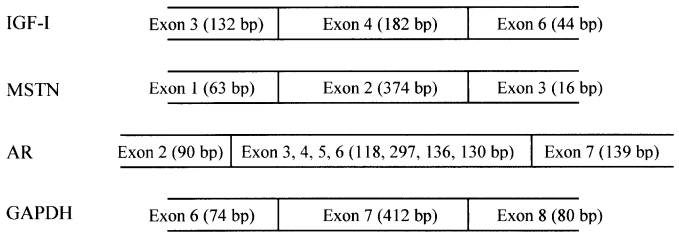

Figure 1. Insulin-like growth factor I (IGF-I), myostatin (MSTN), androgen receptor (AR), and glyceraldehyde-3-phosphate dehydrogenase (GAPDH) clones obtained from amplified ovine sequences all spanned RNA splicing sites in order to control for genomic DNA contamination.

Reverse Transcription-Polymerase Chain Reaction

Construction of a Heterologous Competitor. The relationship between the initial amount A of target mRNA present in the tissue and the amount Y_n of DNA produced after n PCR cycles can be expressed as $Y_n = A \cdot (1 + E)^n$, where E is the amplification efficiency of one

reaction cycle (Chelly et al., 1988). Small variations in reaction efficiency, therefore, translate into large differences in the amount of RT-PCR product generated after *n* cycles. These limitations in quantitative analyses can be overcome by parallel co-amplification of the native mRNA with known amounts of an internal standard cRNA. The amplification efficiency should affect both templates similarly. Several designs have been used in quantitative RT-PCR to obtain an internal standard cRNA that has amplification efficiency identical to that of the native mRNA template and is easily distinguishable from it. One common practice is the use of a PCR MIMIC, a heterologous internal standard that "mimics" the primer binding and amplification characteristics of the target (Gaudette and Crain, 1991; Siebert and Larrick, 1993), obtained with the addition of the specific primers to gene products such as ubiquitously expressed "housekeeping" genes such as GAPDH (Murphy et al., 1990; Gaudette and Crain, 1991).

To quantify ovine muscle and liver IGF-I mRNA abundance by RT-PCR, we constructed a heterologous competitor (MIMIC) based on the ovine GAPDH sequence obtained by RT-PCR using 20 nt primers homologous to ovine GAPDH sequence to which an additional 20 nt were appended on the 5′ ends. The additional 20 nucleotides corresponded to the IGF-I forward and reverse primers, designed based on the ovine IGF-I mRNA sequence (GenBank accession number M31734). These composite primers (Table 1) amplified a 325-bp product, including the 20 bp for IGF-I at both ends. Reverse transcription and amplification techniques were applied to produce first-strand cDNA. Using the Display THERMO-RT Kit (Display Systems Biotech, Boston, MA), 500 μg of total ovine muscle RNA was amplified with an IGFGAPDH reverse primer in the reverse transcription. One microliter of cDNA from the reverse transcription reaction was used in the PCR amplification reaction using the Idaho Technologies Rapid Cycler (Idaho Falls, ID) and the two composite primers (IGFGAPDH forward primer and IGFGAPDH reverse primer). The 325-bp GAPDH MIMIC PCR product was cloned into pCR II using a TA cloning kit (Invitrogen, Carlsbad, CA). The plasmid was subsequently transfected into INVαF′ competent cells (Stratagene, La Jolla, CA). Positive transformants were selected on the basis of ampicillin resistance and, from all positive colonies, 10 were grown in LB broth containing ampicillin (50 μg/μL). The orientation in the plasmid was checked by digestion with *Alu*I restriction enzyme, which has 27 restriction sites in the plasmid and only one in the GAPDH MIMIC. Large-scale plasmid DNA purification was carried out using the Qiagen Plasmid Kit (Valencia, CA). The vector was linearized by *Eco*RV digestion, and the cloned ovine cDNA was transcribed with SP6 RNA polymerase at 37°C for 1 h using the reagents supplied with the MaxiScript kit (Ambion) to create a 422-bp template containing the 325-bp MIMIC and 97 bp of the plasmid. At the end of the reaction, 1 μL of RNase-free DNase I (10 U) was added and the reaction was incubated for 15 min at 37°C. The concentration of RNA MIMIC was determined using spectrophotometry.

Establishment and Validation of the Quantitative RT-PCR. To ensure a parallel start in all individual reactions and to increase specificity, yield, and precision of the PCR, Zombie-Taq (Clontech, Palo Alto, CA) DNA polymerase was used. In the Zombie-Taq DNA polymerase, the polymerase activity is inhibited by the *Taq* antibody until the first denaturation step. To quantify the native IGF-I mRNA in different tissues, a preliminary estimation of the IGF-I cRNA start-molecule concentration range to be used for individual tissues was required. Initially, we titrated against a broad range of dilutions to obtain a rough estimate of the amount of RNA present. This was performed by six titration steps ranging from 2,500 to 0.025 cRNA start-attomoles in a 1:10 dilution scheme added to 0.5 μg of total tissue RNA. We then performed a finer titration over a narrower range of MIMIC (24.1 to 0.1 attomoles for the muscle and 217.2 to 0.9 attomoles for liver in a 1:3 dilution scheme).

Competitive RT-PCR. For each of the three tissues, six RT reactions were performed using 596 ng of total RNA and fixed concentrations of the MIMIC IGF-I cRNA (217.17, 72.39, 24.13, 8.04, 2.68, and 0.89 attomoles for liver and 24.13, 8.04, 2.68, 0.89, 0.30, and 0.1 attomoles for muscle). First-strand cDNA of target and MIMIC were generated using the Omniscript RT Kit (Qiagen, Valencia, CA) in an Amplitron (Barnstead/Thermolyne, Dubuque, IA) thermocycler. The RNA, 1× RT buffer, 0.5 m*M* of each dNTP, 1 μ*M* reverse primer, and 2 U Omniscript Reverse Transcriptase were incubated for 60 min at 37°C. At the end of the reaction, the Omniscript Reverse Transcriptase was inactivated by heating the reaction mixture to 93°C for 5 min followed by rapid cooling on ice. The following PCR was performed in a Rapid Cycler (Idaho Technologies) with 1 μL cDNA; Idaho Technologies buffer (50 m*M* Tris, pH 8.3; 0.25 m*M* crystalline BSA; 2 m*M* $MgCl_2$; and sucrose), 0.4 U *Taq* DNA polymerase (Gibco BRL), 0.2 m*M* dNTPs (Promega), and 0.5 μ*M* each primer. We used 30 cycles (0 s at 94°C, 0 s at 60°C, 15 s at 75°C) followed by an additional 30 s at 75°C for complete amplification of all PCR products. For the Rapid Cycler, 0 s means that the denaturing and annealing temperatures were reached without setting a hold time, because both denaturing and annealing occur almost instantaneously after the sample has reached the appropriate temperature. In each experiment, a negative control, with water replacing template, was included.

Quantification of PCR Products. The 10-μL PCR product was electrophoresed on a 4% NuSieve agarose gel (East Rutherford, NJ), which was then stained in a solution of 0.1 μg/mL ethidium bromide (Figure 2a). The gel was scanned using a gel documentation and

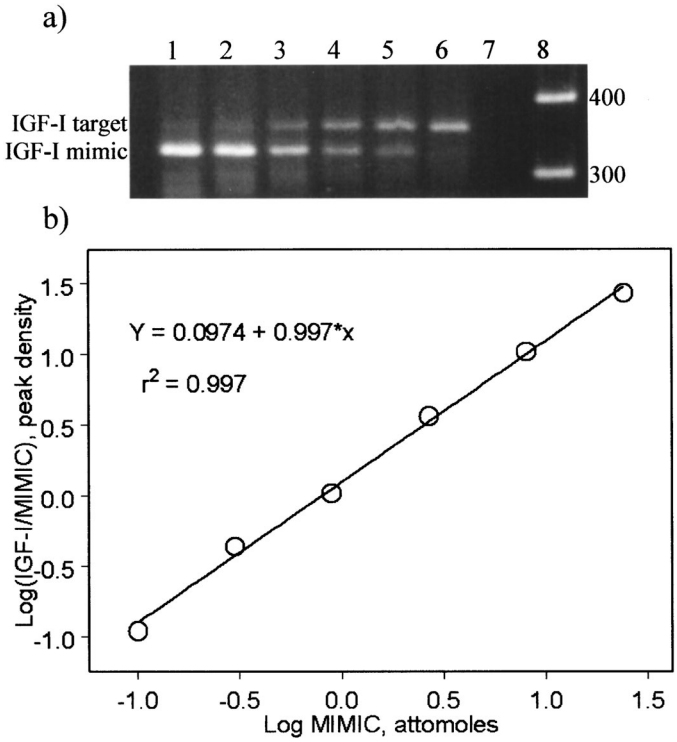

Figure 2. Example of competitive RT-PCR. (a) Total RNA (596 ng) was co-amplified with a dilution series of IGF-I MIMIC cRNA (217.17, 72.39, 24.13, 8.04, 2.68, and 0.89 attomoles for liver and 24.13, 8.04, 2.68, 0.89, 0.30, and 0.1 attomoles for the muscles [lanes 1 through 6]). Lane 7 was a negative control with water replacing template. Lane 8 contained the 100-bp DNA ladder (Life Technology, MD). (b) Following gel electrophoresis and staining with ethidium bromide, the gel was scanned and the density of each peak was integrated. After correcting for size differences, the $\log_{10}$ of the ratio of IGF-I product peak density to IGF-I mimic peak density was plotted against the $\log_{10}$ of the amount of IGF-I MIMIC cRNA added.

analysis system (Alpha Innotech, San Leandro, CA) under UV light. The area of optical densities of the target and the MIMIC peaks were quantified using the Alpha Innotech software. Because the size of the MIMIC cDNA was smaller than the size of the target cDNA, the decrease in the incorporation of ethidium bromide had to be taken into account. The optical density associated with the 325-bp competitor (MIMIC) product was corrected by a multiplication factor corresponding to the base-pair ratio of both fragments as follows:

$$\text{Corrected (band density)} = \text{band density} \times \frac{\text{native bp length}}{\text{competitor (MIMIC) bp length}}$$

The regression of $\log_{10}$ of ratio of the corrected MIMIC band densities to the target band densities (Y variable) against $\log_{10}$ of concentration of the MIMIC (X variable) was performed. As shown in Figure 2b, the association was linear. When the ratio of MIMIC to target was 1 (band densities were equal) the amounts of the target and the MIMIC were equal. To determine the amount of target IGF-I in the sample, we calculated the value of X for a Y value of 0 ($\log_{10}$ 1 = 0).

Statistical Analyses

Our main objective was to compare the gene expression in two specific muscles. Because the two muscles were sampled from each individual, the gene expression of the two muscles represented paired observations with respect to the individual. A new variable was created as the difference between the amount of mRNA expressed in the two muscles for the three genes, D_i = (splenius – semitendinosus)$_i$, where i = 1, 2, …, 11 (animals in the study).

To determine whether age and weight of the animals affected the difference in gene expression in the semitendinosus and splenius muscles, the following regression model was used:

$$D_i = \beta_0 + \beta_1(A_i) + \beta_2(W_i) + \beta_3(AW)_i + e_i$$

where D_i = difference in attomoles/μg RNA between splenius and semitendinosus muscle for the i^{th} animal, A_i = age of the i^{th} animal, W_i = weight of the i^{th} animal, and $(AW)_i$ = age × weight of the i^{th} animal.

Prior to a formal statistical analysis, we plotted the data to assess the type and strength of the relationship. Significant explanatory variables were chosen by a step-down procedure. First, the crossproduct between the two explanatory variables was evaluated and, if not significant, was removed from the model. Second, each explanatory variable was evaluated and, if not significant, was removed from the model.

To test whether there was a difference in gene expression between the two muscles, a hypothesis test was performed. The null hypothesis was H_o: d = 0 and the alternative hypothesis was H_a: d > 0 for IGF-I and AR and H_a: d < 0 for myostatin.

The assumptions of normality and equal variance were checked with a normal probability plot and a plot of the absolute values of residuals against the predicted values.

Results and Discussion

Extractable total RNA was greater ($P < 0.01$) for splenius than for semitendinosus, with 606 and 497 μg RNA/g tissue, respectively. The semitendinosus muscle exhibits a high growth rate during the 1st yr of life, followed by slower growth later in life. A decrease of extractable total RNA concentration in the semitendinosus muscle could be explained by the semitendinosus growth pattern, which is related to hyper-

trophy and dilution of myofiber nuclei and mitochondria. In this context, Arnold et al. (1997) found a decrease of total RNA concentration in semitendinosus compared to splenius with increasing muscle weight of growing lambs. Also, decreased extractable total RNA in semitendinosus with increasing age was shown in cattle (Brandstetter et al., 2000), without any relation to the feeding regimen or castration.

Testosterone

Plasma testosterone concentrations ranged from 0.16 ng/mL to 4.80 ng/mL. The concentrations of testosterone were not correlated with the expression of the three genes investigated. All testosterone concentrations were within the physiological range for rams at this age (Arnold et al., 1997).

Insulin-like Growth Factor I mRNA Expression

Insulin-like growth factor I is a ubiquitous peptide known to stimulate myoblast survival, proliferation, and differentiation (Florini et al., 1995; Stewart and Rotwein, 1996) and it is a potent anabolic agent in regulation of skeletal muscle protein metabolism (Harper et al., 1987; Roeder et al., 1988; Frost et al., 1997).

The IGF-I gene is expressed in many tissues, but liver, and to a lesser extent bone, are the primary sources of circulating IGF-I (Jones and Clemmons, 1995). Several studies have shown that IGF-I can be produced by skeletal muscle, although it is only found at low levels in normal, mature animals (Isgaard, 1992; McGuire et al., 1992). Knock-out mice with a liver-specific IGF-I deletion (Yakar et al., 1999) showed a 75% reduction in IGF-I circulating levels but had normal postnatal and pubertal growth, suggesting that autocrine/paracrine IGF-I production is sufficient for normal growth and development. In all extracellular tissues, IGF-I is bound to a family of six high-affinity IGF-binding proteins (**IGFBP**), designated IGFBP-1 to -6 (Jones and Clemmons, 1995). The IGFBP function not only as carrier proteins for IGF-I in circulation, protecting it from degradation and transporting it to specific tissues, but also as modulators of IGF-I action.

Insulin-like growth factor-I mRNA expression was determined using a competitive RT-PCR, and the mean difference between the splenius and semitendinosus muscles is shown in Table 2. The variation in IGF-I mRNA levels was related neither to age nor to weight of the animals within the ranges covered in the study. The splenius muscle had a higher concentration ($P < 0.05$) of IGF-I mRNA than the semitendinosus muscle (Table 2). The mean difference between the two muscles was statistically significant ($P < 0.05$). This result is consistent with a study of IGF-I gene expression in cattle (Pfaffl et al., 1998a) in which IGF-I mRNA expression was measured in two muscles selected because of their overproportional (splenius) and underproportional (gastrocnemius) growth response to testicular steroids. In bulls, higher IGF-I mRNA concentration was found in the splenius than in the gastrocnemius muscle. Our data support the hypothesis that local differences in IGF-I expression might be one of the mediators of the differential growth of these individual muscles in intact males. However, the concomitant regulation of all other factors of the IGF system, such as the binding proteins and receptors, needs to be considered along with the observed differential regulation of local IGF-I mRNA.

Our results demonstrate that IGF-I mRNA expression in tissues is regulated differently among skeletal muscles as well as among tissues. The highest IGF-I expression was observed in liver, at 17.74 attomoles/μg RNA, which was 20 times higher than in skeletal muscle. This result confirms the importance of the liver as a major site of IGF-I production in postnatal animals (Daughaday and Rotwein, 1989; Rosen and Pollak, 1999) and is in accordance with findings in cattle, in which the hepatic IGF-I mRNA concentrations were 20 to 35 times higher than in skeletal muscle (Pfaffl et al., 1998a).

Androgen Receptor mRNA Expression

The AR is a member of the superfamily of nuclear transcription factors that mediate the action of steroid hormones. When activated by ligand binding, these transcription factors bind to specific DNA sequences on target genes, referred to as *hormone response elements*, and regulate the transcriptional activity of those genes. It is now recognized that unliganded androgen receptors are primarily localized to the cell nucleus (Prins, 2000), and androgens diffuse into the nucleus, where they bind to available receptors.

Testosterone stimulates muscle growth by affecting the rate of protein synthesis, protein breakdown, and the net gain or loss of muscle protein (Rooyackers and Nair, 1997). When testosterone increases muscle protein synthesis, intramuscular mRNA concentrations of IGF-I are increased and concentrations of the inhibitory IGF binding protein 4 are decreased (Urban et al., 1995), and locally produced IGF-I subsequently stimulates muscle protein synthesis and decreases protein breakdown. The response to testosterone differs among muscle groups, and this differential response may be explained by the variation of AR number among skeletal muscles (Krieg et al., 1977). Thus, sexual dimorphism can be explained partly by higher androgen sensitivities in muscles with pronounced growth under androgen stimulation (Sauerwein and Meyer, 1989). A recent study in cattle showed that androgen receptor mRNA concentrations in muscles with different fiber type compositions and growth stimuli is positively related to the individual growth patterns (Brandstetter et al., 2000).

Table 2. Mean mRNA concentration in splenius and semitendinosus muscles and mean and SE of the difference in gene expression between SP and ST muscles (attomoles/μg RNA)

Gene	Splenius	Semitendinosus	Mean difference[a]	SE of the difference	*P*-value
IGF-I	1.39	1.02	0.370	0.200	0.047
Androgen receptor	4.05	2.96	0.975	0.401	0.018
Myostatin	4.29	3.85	0.237	0.582	NS[b]

[a]Mean of the differences; not the difference of the means.
[b]Not statistically significant.

Androgen receptor gene expression in the two muscles showing differential growth patterns was measured by a ribonuclease protection assay (Figure 3) using GAPDH to normalize AR data for differences in RNA loading. Age and weight did not contribute to the variation in AR mRNA levels. Androgen receptor mRNA levels per unit of total RNA measured in splenius were 37% greater than those measured in semitendinosus ($P < 0.05$, Table 2). The increased responsiveness of neck muscles to testosterone could be correlated with the AR level, because changes in the number of receptors are a point of modulation of sensitivity to hormones. Divergent densities of AR in individual muscles have been reported previously in cattle (Sauerwein and Meyer, 1989), and data on the developmental regulation of AR mRNA expression in three bovine muscles that differed in muscle fiber composition, metabolic activity, and growth pattern showed a relationship between AR mRNA concentration and differential growth (Brandstetter et al., 2000). The higher AR mRNA concentrations in splenius muscle shown in this experiment are in agreement with these studies and help to explain the pronounced muscle growth in the neck of maturing rams.

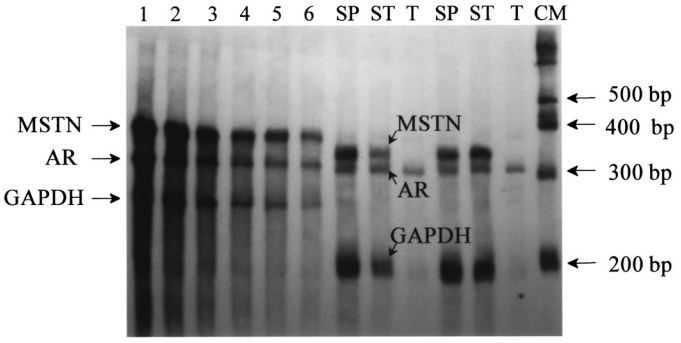

Figure 3. Example of quantitative analyses of myostatin (MSTN) and androgen receptor (AR) mRNA in ovine tissues using GAPDH as an internal control. Lanes 1 to 6 represent a standard curve constructed by hybridizing 1 ng of myostatin, AR and GAPDH antisense probe to 60, 40, 27, 18, 12, and 8 pg of sense myostatin, AR, and GAPDH cRNA, respectively. Lanes ST, SP, and T represents the hybridization of 1 ng myostatin, AR, and GAPDH antisense probe with 40 μg semitendinosus, splenius, and testes RNA, respectively. Testes were included as a control for AR expression. Lane CM represents the RNA molecular weight marker (Century Marker, Ambion). The exposure time varied between 15 and 30 min.

Myostatin mRNA Expression

Myostatin, a member of the transforming growth factor-β superfamily, is specifically expressed in muscle and is a key regulator of skeletal muscle development and growth. Myostatin null mice generated by gene targeting showed a dramatic and widespread increase in skeletal muscle mass. Individual muscles in myostatin null mice weighed two- to threefold more than those of wild-type mice, due to both hyperplasia and hypertrophy (McPherron et al., 1997), without a corresponding increase in the amount of fat. Furthermore, the "double-muscle" phenotypes of three breeds of cattle (Belgian Blue, Piedmontese [Grobet et al., 1997], and Asturiana de los Valles [Dunner et al., 1997]) have been linked to nucleotide deletions, transitions, or transversions within the coding region of the myostatin gene. These mutations likely compromise the biological activity of the protein, which leads to increase muscle mass via hyperplasia and hypertrophy.

The results from myostatin null mice and from double-muscled cattle breeds indicate that lack of myostatin activity during embryonic development allows growth of muscle tissue. There is also increasing evidence that myostatin plays a role in postnatal muscle growth. Myostatin levels are increased in the serum of HIV-infected patients with wasting (Gonzalez-Cadavid, 1998), elderly men and women with sarcopenia (Yarashesky, 1999), and in skeletal muscle in a rat model of aging (Mallidis, 1999) and during hindlimb unloading (Baldwin, 1996).

Recently, myostatin was shown to function by controlling the proliferation of muscle precursor cells (Thomas et al., 2000). Myostatin promotes an increase in p21 expression, a cyclin-dependent kinase inhibitor, and a decrease in Cdk2 protein and activity, thus resulting in an accumulation of hypophosporylated Rb protein. This, in turn, leads to the arrest of myoblasts

in the G1-phase of the cell cycle. Thus, myoblast number and, hence, fiber number, following differentiation, is regulated (limited), suggesting that the increased number of myofibers in cattle and mice with increased muscle mass is a result of deregulated myoblast proliferation caused by the absence of functional myostatin (Thomas et al., 2000).

The RPA measured the presence of myostatin mRNA in both skeletal muscles (Figure 3). No statistically significant difference in myostatin mRNA concentration was found between the splenius and semitendinosus muscles and age and weight of the animals had no effect. We were expecting myostatin gene expression to be lower in the splenius muscle compared to semitendinosus to help explain the increased muscle mass in splenius. Our study did not implicate myostatin in the sexual dimorphism of muscle growth. Nevertheless, myostatin could still play a role in this process, and a study comparing the myostatin gene expression in rams and wethers or in rams before and after puberty might address this issue.

Implications

An increase in IGF-I and AR gene expression could play a role in the increased splenius muscle mass of the neck associated with sexual maturity of rams. However, the regulation of the other components of the IGF-I system should be studied to be able to judge the relevance of the IGF system for regulation of differential muscle growth. Also, the role of AR should be investigated further, because other genes that are regulated by this transcription factor could be associated more directly with muscle growth regulation. Our study showed that myostatin is not implicated in sexually dimorphic muscle growth. Nevertheless, identification and characterization of the myostatin receptor is critical to a complete understanding of the regulatory roles of myostatin.

Literature Cited

Arnold, A. M., J. M. Peralta, and M. L. Thonney. 1996. Ontogeny of growth hormone, insulin-like growth factor-I, estradiol and cortisol in the growing lamb: effect of testosterone. J. Endocrinol. 150:391–399.

Arnold, A. M., J. M. Peralta, and M. L. Thonney. 1997. Effect of testosterone on differential muscle growth and on protein and nucleic acid concentrations in muscles of growing lambs. J. Anim Sci. 75:1495–1503.

Baldwin, K. M. 1996. Effect of spaceflight on the functional, biochemical, and metabolic properties of skeletal muscle. Med. Sci. Sports Exerc. 28:983–987.

Boge, A., H. Sauerwein, and H. H. Meyer. 1995. IGF-I and insulin receptors in bovine skeletal muscle: comparisons of different developmental ages, two different genotypes and various individual muscles. Exp. Clin. Endocrinol. Diabetes 103:99–104.

Brandstetter, A. M., M. W. Pfaffl, J. F. Hocquette, D. E. Gerrard, B. Picard, Y. Geay, and H. Sauerwein. 2000. Effects of muscle type, castration, age, and compensatory growth rate on androgen receptor mRNA expression in bovine skeletal muscle. J. Anim Sci. 78:629–637.

Chelly, J., J. C. Kaplan, P. Maire, S. Gautron, and A. Kahn. 1988. Transcription of the dystrophin gene in human muscle and non-muscle tissue. Nature (Lond.) 333:858–860.

Daughaday, W. H., and P. Rotwein. 1989. Insulin-like growth factors I and II. Peptide, messenger ribonucleic acid and gene structures, serum, and tissue concentrations. Endocr. Rev. 10:68–91.

Dunner, S., C. Charlier, F. Farnir, B. Brouwers, J. Canon, and M. Georges. 1997. Towards interbreed IBD fine mapping of the mh locus: double-muscling in the Asturiana de los Valles breed involves the same locus as in the Belgian Blue cattle breed. Mamm. Genome 8:430–435.

Florini, J. R., D. Z. Ewton, and F. J. McWade. 1995. IGFs, muscle growth, and myogenesis. Diabetes Rev. 3:73–92.

Frost, R. A., C. H. Lang, and M. C. Gelato. 1997. Transient exposure of human myoblasts to tumor necrosis factor-alpha inhibits serum and insulin-like growth factor-I stimulated protein synthesis. Endocrinology 138:4153–4159.

Gaudette, M. F., and W. R. Crain. 1991. A simple method for quantifying specific mRNAs in small numbers of early mouse embryos. Nucleic Acids Res. 19:1879–1884.

Gonzalez-Cadavid, N. F., W. E. Taylor, K. Yarasheski, I. Sinha-Hikim, K. Ma, S. Ezzat, R. Shen, R. Lalani, S. Asa, M. Mamita, G. Nair, S. Arver, and S. Bhasin. 1998. Organization of the human myostatin gene and expression in healthy men and HIV-infected men with muscle wasting. Proc. Natl. Acad. Sci. USA 95:14938–14943.

Grobet, L., L. J. Martin, D. Poncelet, D. Pirottin, B. Brouwers, J. Riquet, A. Schoeberlein, S. Dunner, F. Menissier, J. Massabanda, R. Fries, R. Hanset, and M. Georges. 1997. A deletion in the bovine myostatin gene causes the double-muscled phenotype in cattle. Nat. Genet. 17:71–74.

Harper, J. M., J. B. Soar, and P. J. Buttery. 1987. Changes in protein metabolism of ovine primary muscle cultures on treatment with growth hormone, insulin, insulin-like growth factor I or epidermal growth factor. J. Endocrinol. 112:87–96.

Isgaard, J. 1992. Expression and regulation of IGF-I in cartilage and skeletal muscle. Growth Regul. 2:16–22.

Jones, J. I., and D. R. Clemmons. 1995. Insulin-like growth factors and their binding proteins: biological actions. Endocr. Rev. 16:3–34.

Kambadur, R., M. Sharma, T. P. Smith, and J. J. Bass. 1997. Mutations in myostatin (GDF8) in double-muscled Belgian Blue and Piedmontese cattle. Genome Res. 7:910–916.

Krieg, M., W. Bartsch, S. Herzer, H. Becker, and K. D. Voigt. 1977. Quantification of androgen binding, androgen tissue levels, and sex hormone-binding globulin in prostate, muscle and plasma of patients with benign prostatic hypertrophy. Acta Endocrinol. 86:200–215.

Lee, G. H. Y., M. L. Thonney, and H. M. Richards. 1998. Rapid Communication: Partial clone and sequence of an ovine glyceraldehyde-3-phosphate dehydrogenase cDNA. J. Anim Sci. 76:917.

Mallidis, C., S. Bhasin, A. Matsumoto, R. Shen, and N. F. Gonzalez-Cadavid. 1999. Skeletal muscle myostatin in a rat model of aging-related sarcopenia. In: Proc. Endo. Soc. 81st Annu. Mtg. 73 (OR9-1) (Abstr.).

McGuire, M. A., J. L. Vicini, D. E. Bauman, and J. J. Veenhuizen. 1992. Insulin-like growth factors and binding proteins in ruminants and their nutritional regulation. J. Anim Sci. 70:2901–2910.

McPherron, A. C., A. M. Lawler, and S. J. Lee. 1997. Regulation of skeletal muscle mass in mice by a new TGF-beta superfamily member. Nature (Lond.) 387:83–90.

McPherron, A. C., and S. J. Lee. 1997. Double muscling in cattle due to mutations in the myostatin gene. Proc. Natl. Acad. Sci. USA 94:12457–12461.

Murphy, L. D., C. E. Herzog, J. B. Rudick, A. T. Fojo, and S. E. Bates. 1990. Use of the polymerase chain reaction in the quantitation of mdr-1 gene expression. Biochemistry 29:10351–10356.

Pfaffl, M., H. H. Meyer, and H. Sauerwein. 1998a. Quantification of insulin-like growth factor-1 (IGF-1) mRNA: Development and validation of an internally standardised competitive reverse transcription-polymerase chain reaction. Exp. Clin. Endocrinol. Diabetes 106:506–513.

Pfaffl, M., F. Schwarz, and H. Sauerwein. 1998b. Quantification of insulin-like growth factor-1 (IGF-1) mRNA: modulation of growth intensity by feeding results in inter- and intra-tissue-specific differences of IGF-1 mRNA expression in steers. Exp. Clin. Endocrinol. Diabetes 106:514–521.

Prins, G. S. 2000. Molecular biology of the androgen receptor. Mayo Clin. Proc. 75 Suppl:S32–S35.

Roeder, R. A., K. L. Hossner, R. G. Sasser, and J. M. Gunn. 1988. Regulation of protein turnover by recombinant human insulin-like growth factor-I in L6 myotube cultures. Horm. Metab. Res. 20:698–700.

Rooyackers, O. E., and K. S. Nair. 1997. Hormonal regulation of human muscle protein metabolism. Annu. Rev. Nutr. 17:457–485.

Rosen, C. J., and M. Pollak. 1999. Circulating IGF-I: New Perspectives for a New Century. Trends Endocrinol. Metab. 10:136–141.

Sauerwein, H., and H. H. Meyer. 1989. Androgen and estrogen receptors in bovine skeletal muscle: relation to steroid-induced allometric muscle growth. J. Anim Sci. 67:206–212.

Siebert, P. D., and J. W. Larrick. 1993. PCR MIMICS: competitive DNA fragments for use as internal standards in quantitative PCR. Biotechniques 14:244–249.

Stewart, C. E., and P. Rotwein. 1996. Growth, differentiation, and survival: multiple physiological functions for insulin-like growth factors. Physiol Rev. 76:1005–1026.

Thissen, J. P., J. M. Ketelslegers, and L. E. Underwood. 1994. Nutritional regulation of the insulin-like growth factors. Endocr. Rev. 15:80–101.

Thomas, M., B. Langley, C. Berry, M. Sharma, S. Kirk, J. Bass, and R. Kambadur. 2000. Myostatin, a negative regulator of muscle growth, functions by inhibiting myoblast proliferation. J. Biol. Chem. 275:40235–40243.

Urban, R. J., Y. H. Bodenburg, C. Gilkison, J. Foxworth, A. R. Coggan, R. R. Wolfe, and A. Ferrando. 1995. Testosterone administration to elderly men increases skeletal muscle strength and protein synthesis. Am. J. Physiol 269:E820–E826.

Weimann, E., and W. Kiess. 1990. [Principles and clinical significance of insulin-like growth factors/somatomedins]. Klin. Wochenschr. 68:985–1002.

Yakar, S., J. L. Liu, B. Stannard, A. Butler, D. Accili, B. Sauer, and D. LeRoith. 1999. Normal growth and development in the absence of hepatic insulin-like growth factor I. Proc. Natl. Acad. Sci. USA 96:7324–7329.

Yarasheski, K., S. Bhasin, I. Sinha-Hikim, J. Pak-Loduca, and N. F. Gonzalez-Cadavid. 1999. Serum myostatin-immunoreactive protein concentration is increased with muscle wasting and advanced age. In: Proc. Endo. Soc. 81st Annu. Mtg. 74 (OR92) (Abstr.).